ISSN 1392 - 1207. MECHANIKA. 2009. Nr.1(75)

Experiments and simulations of ultrasonically assisted turning tool

J. Rimkevičienė*, V. Ostaševičius, V. Jūrėnas***, R. Gaidys******

**Kaunas University of Technology, A. Mickevičiaus 37, 44244 Kaunas, Lithuania, E-mail: grazeviciute.jurga@gmail.com*
***Kaunas University of Technology, Studentų 65, 51367 Kaunas, Lithuania, E-mail: vytautas.ostasevicius@ktu.lt*
****Kaunas University of Technology, Kęstučio 27, 44312 Kaunas, Lithuania, E-mail: vytjur@ktu.lt*
*****Kaunas University of Technology, Studentų 50, 51368 Kaunas, Lithuania, E-mail: Rimvydas.Gaidys@ktu.lt*

1. Introduction

The main point in mechanical machining eventually is an increasing of productivity and decreasing of costs at the same time. One of the methods is ultrasonic cutting. This is conventional cutting with applied ultrasonic frequency vibrations to the cutting tool edge.

The cutting tool has the cutting direction and the thrust direction in elliptical vibration mode, so the tool has a velocity component in the chip flow direction in every cutting cycle after it penetrates into the workpiece. The friction force between the tool rake and the chip is effectively reduced by reversing the frictional direction, and the reversed friction force assists the chip to flow out which is much better than using the cutting oil [1].

Ultrasonic assisted tool has no continuous contact with the work piece – that is a reason why average cutting force is lower than at conventional cutting [2]. Friction in the contact is lower, the tool and the work piece have lower thermal influence. Using this method and special inserts [3, 4] good result in mechanical machining of hardened steels can be reached.

Previous research was applied to evaluate the efficiency of ultrasonic cutting tool – comparing it to conventional turning [5]. Next task was to define what kinds of vibrations are the most influent to surface quality of the work piece [6].

In the present work analysis of model adequacy was made – frequency response characteristics were measured and numerically estimated.

The Langevin type transducer [7] consists of piezoceramic elements, the backing (metal cylinder) and the front matching metal horn - cutting tool. The cutting tool and backing were made from grade 45 steel (Young's modulus 210 GPa, density 7850 kg/m^3, poisson's ratio 0.33), as piezoelectric elements two piezoceramic PZT5 rings (Young's modulus 66 GPa, density 7500 kg/m^3, poisson's ratio 0.371) [8] and standard insert CCGT09T304-AlKS05F (Tungaloy) (Young's modulus 360 GPa, density 3900 kg/m^3, poisson's ratio 0.22) were used.

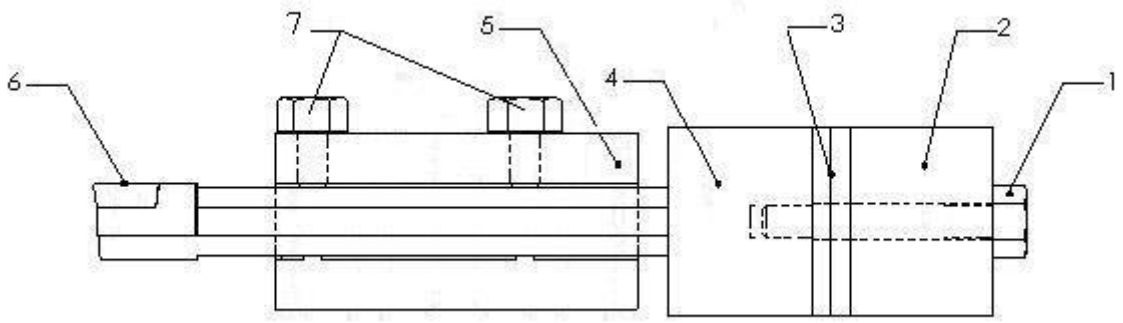

Fig. 1 Scheme of turning tool with holder: *1* – connecting bolt, *2* – backing, *3* – piezoceramic rings, *4* – cutting tool (horn), *5* – tool holder, *6* – insert, 7 – fixing bolts

The tool in the holder is fixed with two bolts (see Fig. 1). The backing *2*, piezoceramic rings *3* and cutting tool (horn) *4* are connected with bolt *1*. Standard insert *6* is fixed in cutting tool.

2. Experimental setup

Experimental setup for measurement of frequency response characteristics is shown in Fig. 2. The tool is fixed in two areas and vibrations are generated with signal generator *3* through power amplifer *2*. Amplitudes on the edge of insert were measured in tree directions (*P* - radial direction to work piece surface, *S* - tangential direction to work piece surface and *F* - vibrations in feed direction) with laser vibrometer *4*. In the vibrometer controller *5* through analog – digital converter *6* the measurement signals were converted and send to the computer *7*. For reading of the signal PicoScope software was used.

The EPA-104 is a high voltage (± 200 Vp), high current (± 200 mA), and high frequency (DC to 250 KHz) amplifier designed to drive higher capacitive (low impedance) loads, such as low voltage stacks, at moderate frequencies; or lower capacitive loads, such as ultrasonic devices, at high frequencies.

Output frequency of the signal generator ESCORT EGC-3235A is from 0.01 Hz to 5 MHz, in 8 Ranges. Amplitude offset is ± 10 V.

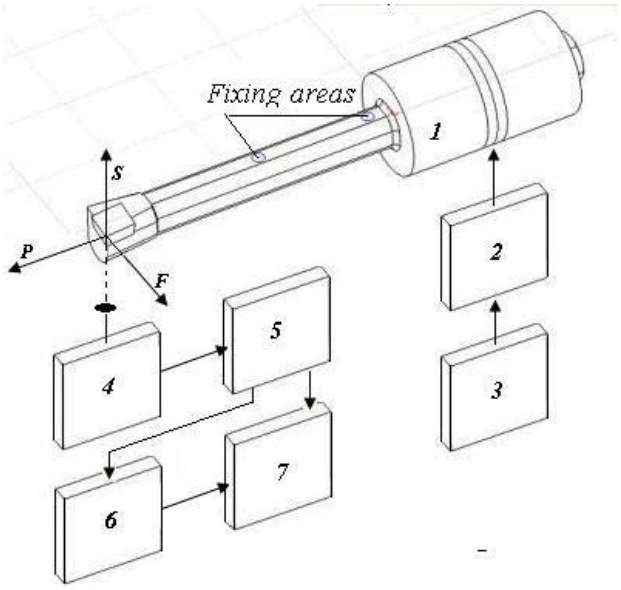

Fig. 2 Experimental setup for measurement of amplitude - frequency characteristics: *1* – vibrator - cutting tool; *2* – power amplifier EPA-104; *3* – signal generator ESCORT EGC-3235A; *4* – laser vibrometer "Polytec "OFV-512"; *5* – vibrometer controller "Polytec OFV-5000", *6* – analog digital converter (ADC) "PicoScope-3424"; *7* – computer

The OFV-5000 controller is designed to accept a choice of signal processing modules, each optimized for different frequency acceleration, velocity or displacement performance.

Vibrations were measured with a laser vibrometer (Polytec Fiber Interferometer OFV 512).

The ADC provides a solution for measuring and recording voltage signals onto PC.

PicoScope is a program, which enables us to use the Pico Technology range of analog to digital converters (ADC) to provide the function of a storage oscilloscope, a spectrum analyser and a digital meter.

In combination with the PicoScope software, the PicoScope-3424 as ADC PC Oscilloscope constitutes a fast, 4-channel memory oscilloscope, a multimeter and a FFT spectrum analyser.

Frequency response curves are shown in Fig. 4, together with numerically estimated curves.

3. Numerical model

Numerical model of experimental cutting tool using finite element software (ANSYS) was made. Material properties of grade 45 steel (horn, connecting bolt and backing), piezoceramic PZT5 (piezoceramic rings) and hardened grade 85W1 steel (insert) were taken.

In linear piezoelectricity the equations of elasticity are coupled to the charge equation of electrostatics by means of piezoelectric constants (IEEE Standard on Piezoelectricity)

$$\begin{bmatrix}\{T\}\\ \{D\}\end{bmatrix}=\begin{bmatrix}[c^E] & [e]\\ [e]^T & -[e^S]\end{bmatrix}\begin{Bmatrix}\{S\}\\ -\{E\}\end{Bmatrix} \tag{1}$$

where $\{T\}$ is stress vector, $\{D\}$ is electric flux density vector, $\{S\}$ is strain vector, $\{E\}$ is electric field intensity vector, $[c^E]$ is elasticity matrix (evaluated at constant electric field), $[e]$ is piezoelectric stress matrix, $[\varepsilon^S]$ is dielectric matrix (evaluated at constant mechanical strain).

The elasticity matrix $[c^E]$ is the usual $[D]$ matrix. It can also be input directly in uninverted form $[c^E]$ or in inverted form $[c^E]^{-1}$ as a general anisotropic symmetric matrix

$$\left[c^E\right]=\begin{bmatrix} c_{11} & c_{12} & c_{13} & c_{14} & c_{15} & c_{16}\\ & c_{22} & c_{23} & c_{24} & c_{25} & c_{26}\\ & & c_{33} & c_{34} & c_{35} & c_{36}\\ Symmetric & & & c_{44} & c_{45} & c_{46}\\ & & & & c_{55} & c_{56}\\ & & & & & c_{66}\end{bmatrix} \tag{2}$$

The piezoelectric stress matrix $[e]$ relates the electric field vector $\{E\}$ in the order X, Y, Z to the stress vector $\{T\}$ in the order X, Y, Z, XY, YZ, XZ and is of the form

$$\left[e\right]=\begin{bmatrix} e_{11} & e_{12} & e_{13}\\ e_{21} & e_{22} & e_{23}\\ e_{31} & e_{32} & e_{33}\\ e_{41} & e_{42} & e_{43}\\ e_{51} & e_{52} & e_{53}\\ e_{61} & e_{62} & e_{63}\end{bmatrix} \tag{3}$$

The piezoelectric matrix can also be input as a piezoelectric strain matrix $[d]$. ANSYS automatically converts the piezoelectric strain matrix $[d]$ to a piezoelectric stress matrix $[e]$ using the elasticity matrix $[c^E]$ at the first defined temperature

$$\left[e\right]=\left[c^E\right]\left[d\right] \tag{4}$$

The dielectric permittivity matrix at constant stress $[\varepsilon^T]$ is of the form

$$\left[\varepsilon^T\right]=\begin{bmatrix}\varepsilon_{11} & 0 & 0\\ 0 & \varepsilon_{22} & 0\\ 0 & 0 & \varepsilon_{33}\end{bmatrix} \tag{5}$$

The anisotropic dielectric matrix at constant stress $[\varepsilon^T]$ is of the form

$$\left[\varepsilon^T\right]=\begin{bmatrix}\varepsilon_{11} & \varepsilon_{12} & \varepsilon_{13}\\ & \varepsilon_{22} & \varepsilon_{23}\\ Symm & & \varepsilon_{33}\end{bmatrix} \tag{6}$$

The dielectric permittivity matrix can also be input as a orthotropic dielectric matrix $[\varepsilon^S]$. It uses the electrical permittivity. The program automatically converts the dielectric matrix at constant stress to a dielectric matrix at constant strain

$$\left[\varepsilon^S\right]=\left[\varepsilon^T\right]-\left[e\right]^T\left[d\right] \tag{7}$$

Numerical scheme is shown in Fig. 3. Fixing areas are modeled as constraint in all directions.

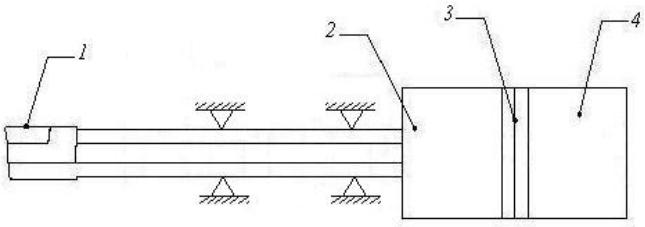

Fig. 3 Numerical scheme of cutting tool: *1* – insert; *2* – cutting tool (horn); *3* – piezoceramic rings; *4* – backing

Equation of motion in matrix form

$$\begin{bmatrix} M_{uu} & 0 \\ 0 & 0 \end{bmatrix} \begin{Bmatrix} \ddot{u} \\ \ddot{\varphi} \end{Bmatrix} + \begin{bmatrix} K_{uu} & K_{u\varphi} \\ K^T & K_{\varphi\varphi} \end{bmatrix} \begin{Bmatrix} u \\ \varphi \end{Bmatrix} = \begin{Bmatrix} F_S \\ Q_S \end{Bmatrix} \quad (8)$$

where $[M_{uu}]$ is mass matrix, $[K_{uu}]$ is mechanical stiffness matrix, $[K_{u\varphi}]$ is piezoelectric coupling matrix, $[K_{\varphi\varphi}]$ is dielectric stiffness matrix, $[F_S]$ is mechanical surface forces – equal to zero, $[Q_S]$ is electrical surface forces.

The system was excited using 100 V voltage and different excitation frequencies.

4. Frequency response

Frequency response curves estimated by experimental measuring (solid) and numerically (dash) are shown in Fig. 4. The curves were estimated in three directions *S*, *F* and *P* (Fig. 2).

In direction *S* the cutting force is biggest one [9], so ultrasonic vibrations in this direction are the most influential.

In Fig. 4 we can see, that superposition of experimentally measured and numerically estimated curves is not satisfactory. The reason of this may be incorrect fixing modeling of the turning tool. That's why the model was updated by modeling elasto-plastic fixing.

Constraint was modeled as the Jenkins element [10], which is an ideal elasto-plastic unit. The sliders are nonlinear elements that implement the Coulomb friction model with a predetermined normal force and coefficient of friction resulting in a break-free force f_i. For a finite number of spring-slider units - n, the force displacement relationship is given by:

$$F(u) = \sum_{i=1}^{n} f_i = \sum_{i=1}^{n} k_i (u - x_i) \quad (9)$$

where x_i is the current displacement of slider i, k_i is stiffness of slider i.

In fixing area springs in each node (Fig. 5) were modeled. Total stiffness value was chosen equal to Young's modulus of grade 45 steel, with a purpose to model the contact correctly.

Modal analysis of the cutting tool was performed. During the analysis of frequency response characteristics it was found out, that dominant peaks correspond the respective modes. Dominant peaks are in directions *S* and *P* at approximately 17 kHz excitation frequency. Here we have the 11th mode with the frequency 17.82 kHz. In Fig. 7 shape of the tool in 11th mode is shown. Here we can see

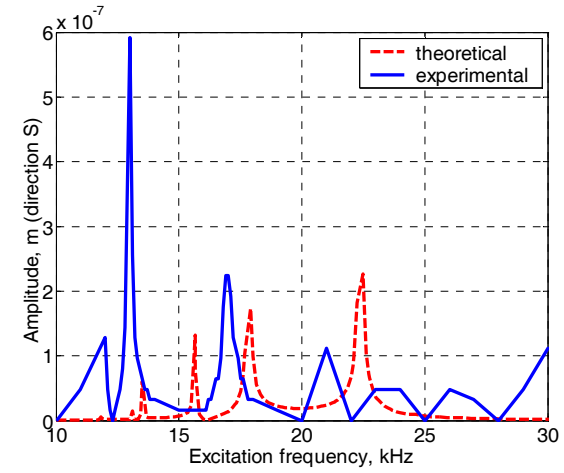

a

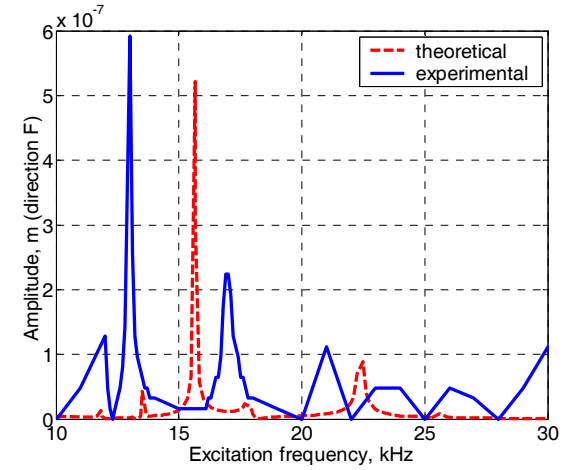

b

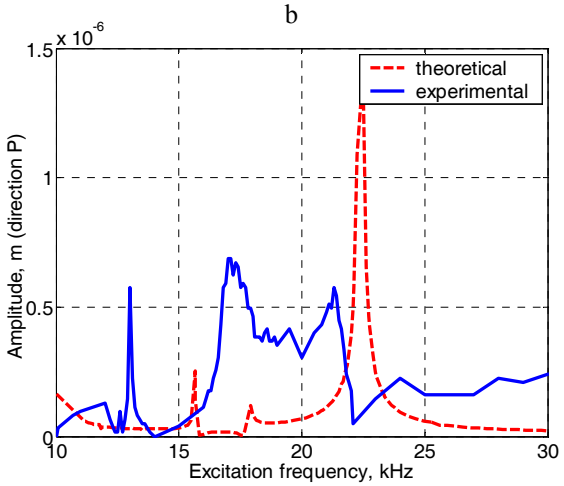

c

Fig. 4 Frequency response characteristics in cutting (*S*), feed (*F*) and radial to the work piece surface (*P*) directions: a - in direction *S*, b – in direction *F*, c – in direction *P*

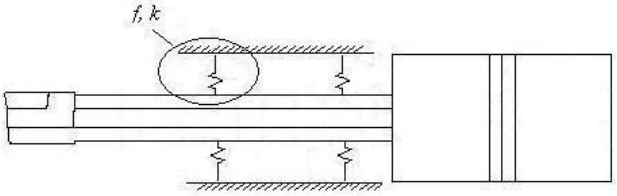

Fig. 5 Numerical scheme of cutting tool, fixing areas are connected to constraints through springs in each node

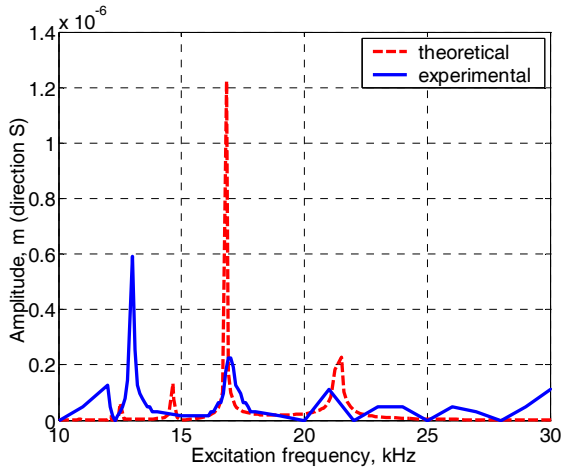

a

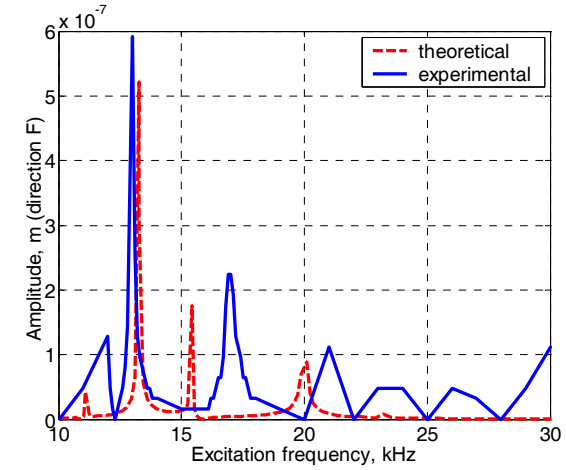

b

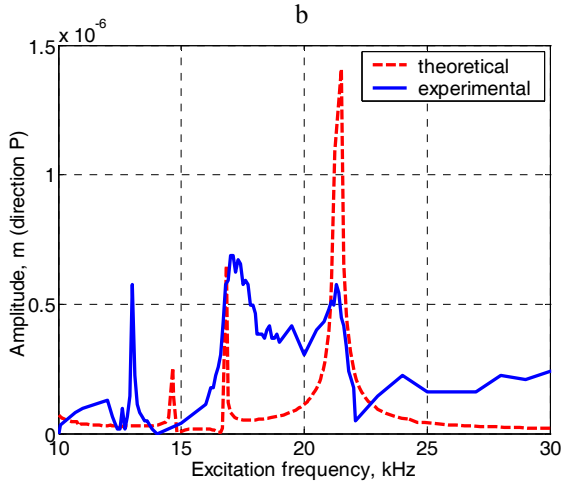

c

Fig. 6 Frequency response characteristics in cutting (*S*), feed (*F*) and radial to work piece surface (*P*) directions after updating the model: a – in direction *S*, b – in direction *F*, c – in direction *P*

that motion is around one area. Cutting edge of the tool is moving around certain area.

Other peaks are at excitation frequency approximately 22 kHz (Fig. 6). According to modal analysis the 12th mode is at excitation frequency 22.39 kHz. The shape of this mode is shown in Fig. 8. Here the cutting tool is vibrating in longitudinal direction.

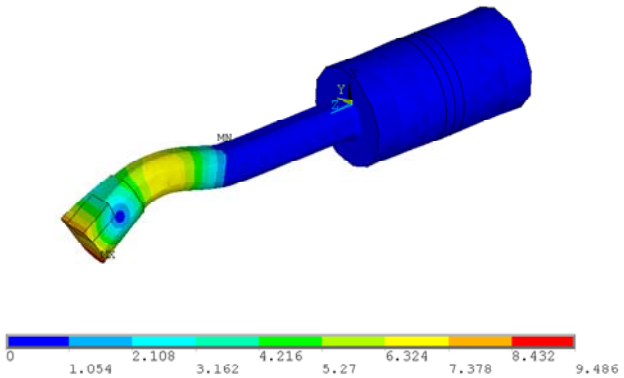

Fig. 7 Deformed shape of 11th mode, frequency 17.82 kHz

After this analysis the conclusion can be made, that: for exiting longitudinal vibrations and vibrations in cutting direction is purposeful to excite 11th and 12th modes of the cutting tool.

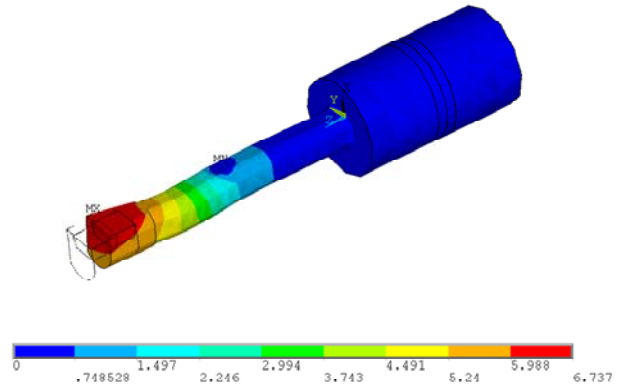

Fig. 8 Deformed shape of 12th mode, frequency 22.39 kHz

5. Conclusions

1. Frequency response characteristics of experimental measurement and numerically estimated are superposed, when boundary conditions of the tool is modeled as elasto-plastic.

2. Numerical model is adequate and can be used in further research of turning tool dynamics.

References

1. **Li, Xun, Zhang, Deyuan.** Ultrasonic elliptical vibration transducer driven by single actuator and its application in precision cutting. -J. of Materials Processing Technology, 2006, 180, p.91-95.
2. **Kim, Gi Dae, Loh, Byoung Gook.** Characteristics of elliptical vibration cutting in micro-V grooving with variations in the elliptical cutting locus and excitation frequency. -J. of Micromechanics and Microengineering, 2008, 18, p.12.
3. **Bouchelaghem, H., Yallese, M.A., Amirat, A., Belhadi, S.** Wear behaviour of CBN tool when turning hardened AISI D3 steel.-Mechanika.-Kaunas: Technologija, 2007, Nr.3(65), p.57-65.
4. **Fnides, B., Yallese, M.A., Aouici, H.** Hard turning of hot work steel AISI H11: Evaluation of cutting pressures, resulting force and temperature.-Mechanika. -Kaunas: Technologija, 2008, Nr.4(72), p.59-63.

5. **Graževičiūtė, J., Skiedraitė, I., Ostaševičius, V., Jūrėnas, V., Bubulis, A.** Ultrasonic application in turning process.-Proc. of the 6th Int. Conf. "Vibroengineering 2006", October 12-14, 2006, Kaunas, 2006, p.152-154.
6. **Graževičiūtė, J., Skiedraitė, I., Ostaševičius, V., Jūrėnas, V., Bubulis, A.** Influence of turning tool dynamics on surface quality of work piece. -Proc. of 13th Int. Conf. "Mechanika 2008", April 3-4, 2008, Kaunas, 2008, p.149-152.
7. **Iula, A., Lamberti, N., Pappalardo, M.** FE analysis of a high displacement ultrasonic actuator based on a flexural mechanical amplifier.-19th Int. Congress on Acoustics.-Madrid, September 2007, p.2-7.
8. **Ju Hyun Yoo, Jae Il Hong, Wenwn Cao**. Piezoelectric ceramic bimorph coupled to thin metal plate as cooling fan for electronic devices.-Sensors and Actuators 79, an Int. J. Devoted to Research and Development of Physical Transducers, 2000, p.8-12.
9. **Vergnas J.** Usinage. Technologie et pratique. -Metz, France, 2001, p.16-19 (in French).
10. **Songa, Y., Hartwigsenb, C.J., McFarlanda, D.M., Vakakisb, A.F., Bergmana, L.A.** Simulation of dynamics of beam structures with bolted joints using adjusted Iwan beam elements.-J. of Sound and Vibration, 2004, 273, p.249-276.

J. Rimkevičienė, V. Ostaševičius, V. Jūrėnas, R. Gaidys

ULTRAGARSU ŽADINAMO TEKINIMO PEILIO EKSPERIMENTAI IR MODELIAVIMAS

R e z i u m ė

Straipsnyje pateikti ultragarsu žadinamo tekinimo peilio eksperimentiniai ir modeliavimo tyrimai. Modeliuodami nejudamą peilio įtvirtinimą matome, kad modeliuotos atsako į harmoninį žadinimą amplitudės yra pasislinkusios dažnio didėjimo kryptimi, palyginti su eksperimentinėmis, rezonansiniai žadinimo dažniai nesutampa keletu kilohercų. Nustatyta, kad modelis adekvatus, t. y. eksperimentinių ir modeliavimo priklausomybių rezonansiniai dažniai sutampa, sumodeliavus ne standų įtvirtinimą, o tamprų, kai kiekviename prispaudimo ploto mazge modeliuojamos spyruoklės, o suminis jų standumas parenkamas lygus plieno 45 Jungo moduliui.

J. Rimkevičienė, V. Ostaševičius, V. Jūrėnas, R. Gaidys

EXPERIMENTS AND SIMULATIONS OF ULTRASONICALLY ASSISTED TURNING TOOL

S u m m a r y

This paper presents the experimental and simulation investigation of ultrasonically assisted turning tool. By modeling of immovable fixing of tool we see, that the amplitudes of simulated frequency response are shifted towards frequency increasing comparing with experimental ones, and resonant excitation frequencies do not match in few kilohertz. It was estimated, that the model is adequate (experimental and simulated resonant frequencies are close), when fixing is modeled as elasto-plastic, and in each node of fixing area springs are modeled, total stiffness of them is chosen equal to Young's modulus of grade 45 steel.

Ю. Римкявичене, В. Осташявичюс, В. Юренас, Р. Гайдис

ЭКСПЕРИМЕНТАЛЬНЫЕ ИССЛЕДОВАНИЯ И МОДЕЛИРОВАНИЕ ТОКАРНОГО РЕЗЦА С УЛЬТРАЗВУКОВЫМ ВОЗБУЖДЕНИЕМ

Р е з ю м е

В настоящей работе приведены экспериментальные исследования и моделирование токарного резца с ультразвуковым возбуждением. Моделированием жестко закрепленного резца определены резонансные частоты, которые превышают резонансные частоты резца, измеренные экспериментальными исследованиями, на несколько килогерц. Установлено, что резонансные частоты модели упруго закрепленного резца с точечным закреплением в виде пружин, имеющих коэффициент упругости равный модулю Юнга стали марки 45, лучше совпадают с резонансными частотами резца, измеренными экспериментально.

Received December 02, 2008
Accepted February 12, 2009